Manuscript Details

Manuscript number	EFA_2018_415_R1
Title	FAILURE ANALYSIS OF WORN VALVE TRAIN COMPONENTS OF A FOUR-CYLINDER DIESEL ENGINE
Article type	Research Paper

Abstract

This work investigates the causes of excessive wear occurring at the rocker arm/pushrod and rocker arm/valve interfaces of a diesel engine for industrial cleaning machines, after only 1000 hours of engine operation. In this engine, the recent replacement of tappets by hydraulic valve lifters not only reduced the running time but also required supplementary maintenance. The chemical composition of the worn components was verified by optical emission spectroscopy. The microstructures, mechanical properties and surface textures were determined by optical microscopy, Vickers hardness and non-contact 3D profilometry. To evaluate the wear mechanisms, the worn surfaces were analyzed by scanning electron microscopy with energy dispersive spectroscopy. The results indicated non-uniform wear damage at the rocker arm/valve interface, probably due to a misalignment of valves with respect to valve seat inserts. For rocker arms and pushrods, improper austenitization parameters and/or unsuitable design of the inductor left some free ferrite, responsible for non-compliance with required specifications for the induction hardening treatment. All worn surfaces were characterized by material removal by scuffing; initiation of fatigue cracks was also observed at the rocker arm/valve interface, and probably erosive cutting occurred at the rocker arm/pushrod interface.

Keywords	Failure analysis; Diesel engine; Microstructures; Scuffing; SEM/EDS.

Corresponding Author	CHIARA SOFFRITTI
Order of Authors	CHIARA SOFFRITTI, Mattia Merlin, REYNA VAZQUEZ-AGUILAR, Annalisa Fortini, Gian Luca Garagnani

Suggested reviewers	Omar Es-Said, Lawrence Eiselstein

Submission Files Included in this PDF

File Name [File Type]

Soffritti et al_Cover Letter_Revised.docx [Cover Letter]

Soffritti et al_Response to Reviewers.doc [Response to Reviewers]

Soffritti et al_ Highlights.docx [Highlights]

Soffritti et al_Manuscript_Revised.docx [Manuscript File]

Soffritti et al_Fig1.tiff [Figure]

Soffritti et al_Fig2.tiff [Figure]

Soffritti et al_Fig3.tiff [Figure]

Soffritti et al_Fig4.tiff [Figure]

Soffritti et al_Fig5.tiff [Figure]

Soffritti et al_Fig6.tiff [Figure]

Soffritti et al_Fig7.tiff [Figure]

Soffritti et al_Fig8.tiff [Figure]

Soffritti et al_Fig9.tiff [Figure]

Soffritti et al_Fig10.tiff [Figure]

Soffritti et al_Fig11.tiff [Figure]

Soffritti et al_Table1.docx [Table]

Soffritti et al_Table2.docx [Table]

Soffritti et al_Table3.docx [Table]

Soffritti et al_Table4.docx [Table]

To view all the submission files, including those not included in the PDF, click on the manuscript title on your EVISE Homepage, then click 'Download zip file'.

UNIVERSITÀ DEGLI STUDI DI FERRARA
- EX LABORE FRUCTUS -

DE Department of Engineering Ferrara

To the Editors of
Engineering Failure Analysis

Subject: Revision of manuscript EFA_2018_415

Dear Sirs,

Thank you very much for your mail and for kindly providing comments and/or suggestions on our manuscript (EFA_2018_415). We carefully amended the manuscript according to the suggestions provided and enclose a detailed answer to the Reviewers' comments. We hope now that the manuscript is suitable for publication on your Journal.

Thank you for your kind attention and best regards,

Chiara Soffritti, PhD
Corresponding author

Department of Engineering
University of Ferrara,
Via Saragat 1, 44122 Ferrara (Italy)
E-mail: chiara.soffritti@unife.it

Ferrara, May 28th, 2018

ANSWERS TO THE REVIEWERS:

REVIEWER 1

This is an interesting paper concerned with the failure of worn valve train components of diesel engine. The components failed by excessive wear and the failure was influenced by material removal by scuffing and probably also by erosive cutting caused by free moving particles transported by the lubricant.
The paper is well written and is topical. The quality of English is good, with few or no significant grammatical errors. The conclusions are well written and are supported by the evidence presented. The paper makes an interesting and reasonably complete case study that is useful to workers in the field.
I recommend that the paper be accepted without alteration.

We thank the Reviewer for his/her favorable comments and his/her positive evaluation. We are glad for his/her appreciation of our study.

REVIEWER 2

Some minor editorial issues for instance:

274-275 "…up, producing wear particles and pits [16,22]. The intermittent propagation of fatigue cracks during each cycle has been observed in this study by the presence of fatigue striations inside pits. In all…". There one fatigue striation does not necessarily mean one load cycle. This may be better stated as "Fatigue cracking was identified by the presence of fatigue striations that indicate the periodic advance of the crack front during cyclic loading.".

Following the Reviewer's suggestion, we amended the sentence as follows:

"...up, producing wear particles and pits [16,22]. Fatigue cracking has been identified by the presence of fatigue striations inside pits that indicate the periodic advance of the crack front during cyclic loading. In all…".

298 - "…the permanence of free ferrite at the induction hardened regions of rocker arms favors the..." I believe permanence should actually be presence.

According to the Reviewer's suggestion, we amended the sentence as follows:

"...the presence of free ferrite at the induction hardened regions of rocker arms favors the…".

Highlights

- Excessive wear was detected in valve train components of a diesel engine.
- The cause was probably misalignment of valves with respect to valve seat inserts.
- The induction hardened regions of rocker arms and pushrods contained free ferrite.
- Scuffing and pits were detected at the rocker arm/valve interface.
- Scuffing and probably erosive cutting occurred at the rocker arm/pushrod interface.

FAILURE ANALYSIS OF WORN VALVE TRAIN COMPONENTS OF A FOUR-CYLINDER DIESEL ENGINE

C. Soffritti[a,*], M. Merlin[a], R. Vazquez[a], A. Fortini[a], G.L. Garagnani[a]

[a] Department of Engineering, University of Ferrara, Via Saragat 1, I-44122 Ferrara, Italy

* Corresponding author
Department of Engineering
Via Saragat 1, I-44122 Ferrara, Italy
Tel. +39 0532 974843
Fax +39 0532 974870
e-mail: chiara.soffritti@unife.it

Co-authors addresses: mattia.merlin@unife.it, vzqrnr@unife.it, annalisa.fortini@unife.it, gian.luca.garagnani@unife.it.

Abstract

This work investigates the causes of excessive wear occurring at the rocker arm/pushrod and rocker arm/valve interfaces of a diesel engine for industrial cleaning machines, after only 1000 hours of engine operation. In this engine, the recent replacement of tappets by hydraulic valve lifters not only reduced the running time but also required supplementary maintenance. The chemical composition of the worn components was verified by optical emission spectroscopy. The microstructures, mechanical properties and surface textures were determined by optical microscopy, Vickers hardness and non-contact 3D profilometry. To evaluate the wear mechanisms, the worn surfaces were analyzed by scanning electron microscopy with energy dispersive spectroscopy. The results indicated non-uniform wear damage at the rocker arm/valve interface, probably due to a misalignment of valves with respect to valve seat inserts. For rocker arms and pushrods, improper austenitization parameters and/or unsuitable design of the inductor left some free ferrite, responsible for non-compliance with required specifications for the induction hardening treatment. All worn surfaces were characterized by material removal by scuffing; initiation of fatigue cracks was also observed at the rocker arm/valve interface, and probably erosive cutting occurred at the rocker arm/pushrod interface.

Keywords: Failure analysis; Diesel engine; Microstructures; Scuffing; SEM/EDS

1. Introduction

Diesel engines for industrial machines generally undergo heavy using conditions, thus wear may quickly jeopardize their functions unless carefully monitored and controlled. From a tribological point of view, since 1950 the use of more efficient fuels and compact engines with low environmental impact caused an increase of specific loads, operative velocity and temperature of all components subject to wear and friction. Moreover, the use of low-viscosity lubricating oils necessarily has led to a reduction of lubricating film thickness between the contact surfaces in reciprocating sliding motion [1]. The cost of diesel engines has been greatly affected by the increasing demand for long duration and prolonged maintenance intervals [2,3]. The increasing request by laws and customers for abatement of pollutant emissions has also favored the development of several technologies to eliminate soot, mostly produced by obstruction of injectors and accumulation of carbon particles in manifolds [4]. Soot particulate emissions are known to reduce wear and fatigue resistance of diesel engine components due to the interactions between soot, metal and lubricant additives or among soot particles [5-8].

Recently, modeling and simulation in engine designing have emerged as important tools for optimizing and predicting wear of mechanical systems under variable load and/or sliding speed. For example, a model of rigid body mechanics was used to simulate the contact between the rocker arm pad and the valve bridge in the cam mechanism of a diesel engine: the results showed that the radius and the center position of the wear pad influenced the maximum wear depth and distribution [9]. When a re-design of the tribological system is required, it is advisable to perform a control of the wear mechanism in real components, where the main cause of failure is faulty manufacturing involving cracks, stress concentration or improper heat treatments. The failure analysis of two rocker arms from heavy duty diesel engines [10] showed a banded microstructure and the spheroidization of cementite in pearlite, deriving from an unsuitable normalizing heat treatment. These metallurgical defects lowered fatigue strength and favored initiation and growth of fatigue cracks with multiple origins. Another study attributed to stress concentration the failure by fatigue of a diesel engine rocker arm [11].

The present study investigates the causes of excessive wear occurring at rocker arm/pushrod and rocker arm/valve interfaces of a diesel engine for industrial cleaning machines. In this engine, the recent replacement of tappets by hydraulic valve lifters not only reduced the running time but also required supplementary maintenance. The chemical composition of the worn components was determined by optical emission spectroscopy (OES) and the microstructures were identified by optical microscopy (OM). Vickers hardness and surface texture measurements were also performed. Finally, to determine the wear mechanisms the worn surfaces were studied at high magnification by scanning electron microscopy with energy dispersive spectroscopy (SEM/EDS).

2. Material and methods

Four pairs of rocker arms, pushrods and valves were collected from a four-cylinder diesel engine for industrial cleaning machines. In this engine, all clearances at the induction hardened regions were set back to zero due to excessive wear after only 1000 hours of engine operation. A schematic representation of the outlet/inlet rocker arm and parts of the pushrod and exhaust/intake valve is shown in Fig. 1, together with an indication of the regions with worn surfaces. The outlet/inlet rocker arm, pushrods and the exhaust and intake valves were prepared for analysis of the chemical composition of the steel types by optical emission spectroscopy (OES) through a SPECTROLAB analyzer (SPECTRO Analytical Instruments GmbH, Kleve, Germany). The details of chemical composition of the different steel types are shown in Table 1. In order to increase surface hardness and contact fatigue resistance, in this engine some regions of the outlet/inlet rocker arm pad, the outlet/inlet rocker arm pivot socket, the pushrod ball ends and the exhaust/intake valve stem tip were induction hardened. The required specifications concerning Rockwell hardness values (HRC) and effective depth of the regions undergoing induction hardening treatment are shown in Table 2. The worn surfaces were first observed by a Leica MZ6 (Leica, Wetzlar, Germany) stereomicroscope. To determine the microstructures of alloys, longitudinal sections (parallel to the metal surface) and cross-sections (perpendicular to the metal surface) of the samples were prepared, mounted in resin, polished and analyzed by a Leica MEF4M optical microscope (Leica). Microstructural investigations were carried out after chemical etching by Nital 4 (4% nitric acid in ethanol) under the same optical microscope. The micrographs of the cross-sections were processed by Leica Application Suite (LAS, Leica) image analysis software to evaluate the area fraction of metallographic phases occurring in the induction hardened regions. A mean of 15 micrographs were analyzed for each component. On the cross-sections, Vickers hardness measurements (HV1) under 1000 g_f load and 15 s loading time were performed in triplicate at increasing distances from the worn surfaces (0.2-4.0 mm) by a Future-Tech FM-110 Vickers microindenter (Future-Tech Corp., Kawasaki, Japan). The Vickers hardness values were then converted in Rockwell hardness values according to the standard ASTM E140-12 to verify the required specifications for the induction hardening treatment.

The 3D surface textures of the outlet/inlet rocker arm pads and exhaust/intake valve stem tips were evaluated by a Talysurf CCI-Lite non-contact 3D profilometer (Taylor-Hobson, Leicester, UK). The 3D height parameters Sa (arithmetical mean height of the surface), Sq (root mean square height of the surface), Ssk (skewness) and Sku (kurtosis) were determined according to the standard ISO 25178. Each value was an average of twenty measurements performed on 1.0x1.0 mm^2 areas of both fresh and worn surfaces. To identify the wear mechanisms the worn surfaces were characterized by a Zeiss EVO MA 15 (Zeiss, Oberkochen, Germany) scanning electron microscopy (SEM), equipped with an Oxford X-Max 50 (Oxford Instruments, Abingdon-on-Thames, UK) energy dispersive microprobe for semi-quantitative analyses (EDS). The SEM micrographs were recorded in secondary electron imaging (SEI-SEM) and back-scattered electron (BSE-SEM) mode.

3. Results

The stereomicroscopy images representing the excessive wear at the induction hardened regions are shown in Fig. 2a-f. The extent of wear on the surface of the outlet rocker arm pad (Fig. 2(a)) was greater than that on the surface of the inlet rocker arm pad (Fig. 2(b)). At the exhaust side, the wear damage was slightly offset from the center of the outlet rocker arm pad; conversely, at the intake side, the wear damage was located at the center of the inlet rocker arm pad. At exhaust and intake sides, the depth of wear was higher at the surface regions respectively located at the opposite directions of the intake and of the exhaust side (white arrows in Fig. 2(a) and (b)). From a morphological point of view, the worn surface of the outlet/inlet rocker arm pad could be divided into two zones: the first one (Fig. 2(a), red outline) was shiny with scuffing appearance, whereas the second one (Fig. 2(a), orange outline) was matted with numerous pits uniformly distributed over the worn surface. Moreover, on the worn surface of the inlet rocker arm pad (Fig. 2(b)) several concentric circles were visible. The morphology of the worn surfaces of exhaust and intake valve stem tips was characterized by the same features observed on the worn surface of the outlet/inlet rocker arm pad (Fig. 2(c) and (d)). Once again, at the center of the intake valve stem tip many concentric circles could be observed (Fig. 2(d)). Concerning the outlet and inlet rocker arm pivot sockets, excessive wear involved material removal with grooves and scratch marks, mostly parallel and distributed over the worn surfaces (Fig. 2(e) and (f)).

An example of the microstructure observed on the cross-section of the inlet rocker arm pivot socket is shown in Fig. 3a-c. Beginning from the worn surface inwards, the microstructure of the induction hardened region was bainitic-martensitic with some free ferrite (Fig. 3(a)), and that of the transition region between the induction hardened layer and the unaffected core was upper bainitic with troostite, again with some free ferrite (Fig. 3(b)). The coarse microstructure of the unaffected core was ferritic-pearlitic (Fig. 3(c)). The microstructures of the cross-sections of the outlet rocker arm pivot socket and of the outlet/inlet rocker arm pad were similar. The pushrod ball ends were totally induction hardened, thus the microstructure was uniformly bainitic-martensitic with some free ferrite. The mean area fractions in percentage of bainite-martensite and free ferrite occurring in the induction hardened regions of the outlet/inlet rocker arm pad, outlet/inlet rocker arm pivot socket and pushrod ball ends are shown in Table 3. The area fraction of free ferrite was the highest ($\cong$10%) in the outlet/inlet rocker arm pivot socket, while in the outlet/inlet rocker arm pad and pushrod ball ends ranged from 3 to 6%.

An example of the banded microstructure observed on a cross-section of the intake valve stem tip is shown in Fig. 4a-b. The microstructure of the induction hardened region was martensitic with large primary carbides oriented along the working direction and small secondary carbides located along the grain boundaries (Fig. 4(a)). The microstructure of the unaffected core was composed of fine pearlite and globular cementite particles, with a greater amount of oriented large primary carbides and segregated secondary carbides (Fig. 4(b)). The microstructures of the cross-sections of the exhaust valve stem tip were similar.

The Vickers hardness profiles of the cross-sections of inlet rocker arm pad, inlet rocker arm pivot socket, pushrod ball ends, exhaust valve stem tip and intake valve stem tip at different distances from the worn surfaces are displayed in Fig. 5a-e. For the inlet rocker arm pad and inlet rocker arm pivot socket, the hardness profiles did not comply with the specifications concerning HRC values and effective depth required at the induction hardened regions: for the inlet rocker arm pad, the required HRC values (55-59 HRC, corresponding to 595-674 HV1) were maintained only up to about 0.5 mm in depth (Fig. 5(a)); for the inlet rocker arm pivot socket (Fig. 5(b)), the HRC values were not the required ones and no decrease in hardness was registered from the worn surface to the core of material. Moreover, the hardness profile of the inlet rocker arm pivot socket (Fig. 5(b)) showed marked discontinuities between 1.1 and 2.6 mm in depth. Overall, the Vickers hardness profiles showed that HRC values and effective depth were below the required specifications for all pairs of rocker arms.

The Vickers hardness values of cross-sections of all pushrods (Fig. 5(c)) were more or less constant, but the related HRC values were below the minimum requirement for the induction hardened region (58 HRC, corresponding to 653 HV1).

For all exhaust and intake valves (Figs. 5(d) and (e)), the HRC values and effective depth at the induction hardened regions satisfied the required specifications.

Examples of 3D surface textures of the worn surfaces of the outlet/inlet rocker arm pad and exhaust/intake valve stem tip are shown as 3D isometric views in Fig. 6a-d. The 3D isometric view of the surface of the inlet rocker arm pad was apparently less worn in comparison to that of the other three components. The mean values of the 3D height parameters Sa, Sq, Ssk and Sku of the fresh and worn surfaces of the outlet/inlet rocker arm pad and exhaust/intake valve stem tip are shown in Table 4. For the outlet rocker arm pad and the exhaust/intake valve stem tip, the Sa and Sq values of the worn surfaces were higher than those of the fresh ones; on the contrary, as previously mentioned, those of the inlet rocker arm pad were lower than those of the fresh ones. The skewness (Ssk) of the fresh surfaces was negative, but that of the worn surfaces became positive for all components except the exhaust valve stem tip. Concerning the kurtosis (Sku), this parameter exhibited a different behavior: for the outlet/inlet rocker arm pad, Sku values of the fresh surfaces were higher than those of the worn surfaces (Sku < 3.00), but those of the exhaust/intake valve stem tip were lower than those of the worn surfaces (Sku > 3.00).

The SEI-SEM micrographs of the worn surfaces of pushrod ball ends are shown in Fig. 7a-c. The morphology of the worn surface of pushrod ball ends (Fig. 7(a)) was characterized by two features: material removal by scuffing (Fig. 7(b)) and probably by erosive cutting (Fig. 7(c)). The material removal by scuffing was associated with linear grooves and scratch marks, mostly parallel and uniformly distributed over a wide area of the worn surface. All plastically deformed material was mostly removed by the surface during motion and to a minor extent it accumulated to the sides of the grooves. The erosive cutting generated a series of ripples oriented along the direction of grooves and limited to a narrow region of the worn surface. For all pairs of pushrod ball ends and rocker arm pivot sockets the morphology of the worn surfaces was similar.

The SEM/EDS analysis of the shiny area observed on the worn surface of outlet rocker arm pad (Fig. 2(a)) indicated material removal by scuffing, as in pushrod ball ends. Concerning the matted area observed on the worn surface of the same component, the SEI-SEM micrographs showed the presence of numerous pits, ranging in size from a few tens of micrometers to several hundred micrometers (Fig. 8(a)). At higher magnification, subsurface interconnected microcracks and fatigue striations were visible inside the pits (Fig. 8(b)), together with wear particles in the form of spherical agglomerates (Fig. 9 (left)). The semi-quantitative EDS analysis of spherical agglomerates indicated the presence of high percentages of oxygen and iron, and traces of manganese, silicon and calcium (Fig. 9 (right)). For all pairs of outlet/inlet rocker arm pads the morphology of the worn surfaces was similar.

The morphology of the worn surfaces of all pairs of exhaust/intake valve stem tips was characterized by the same features identified on the worn surfaces of the outlet/inlet rocker arm pads, but the grooves, scratch marks and pits were less marked (Figs. 10(a) and (b)).

These worn surfaces were also analyzed by SEM/EDS in back-scattered electron mode (BSE-SEM), followed by semi-quantitative EDS analysis. In all surfaces, dark and light contrast areas could be identified (Fig. 11 (left)): the EDS analysis revealed the presence of sulfur, phosphorous, calcium and zinc in the dark contrast areas, which was related to the residues of lubricant additives (Fig. 11 (right)).

4. Discussion

A failure analysis process was performed to investigate the excessive wear occurring at rocker arm/pushrod and rocker arm/valve interfaces of a diesel engine for industrial cleaning machines. The worn surfaces of the outlet rocker arm pad show a high wear damage due to the harsh chemical environment and high temperatures occurring at the exhaust side. For the outlet/inlet rocker arm pad, the position of the wear tracks and the higher wear depth at the surface regions located at the opposite direction of the intake/exhaust side suggest a misalignment of the valves with respect to the valve seat inserts. The role of valve seat insert is to avoid direct contact of the valve with the cylinder head, absorbing part of the combustion heat transferred to the valve and passing it onto the cylinder head [12]. Slight misalignments caused by small differences in roundness or valve seating face angles may lead to uneven wear and non-uniform heat transfer from the valve head to the seat insert. Eventually, misalignments occurring during assemblage may cause the valve recession into the seat insert [13,14]. The absence of concentric circles on the wear surfaces of the outlet rocker arm pad and exhaust valve stem tip, associated to non-rotating valve during engine operation, support the hypothesis of misalignment, although the concentric circles could have been removed by scuffing at the rocker arm/valve interface. On the other hand, the concentric circles are visible on the worn surfaces of the inlet rocker arm pad and intake valve stem tip, thus the valve rotates more or less correctly, reducing wear and friction [15].

The optical microscope images show some free ferrite at the induction hardened regions of the outlet/inlet rocker arm and pushrods. The outlet/inlet rocker arm pivot socket contained the highest percentage of free ferrite (≅10%), while the outlet/inlet rocker arm pad and pushrod ball ends had percentages ranging from 3 to 6%. The induction hardening treatment should involve a rapid austenitization of the surface of a steel part through the magnetic field of a water-cooled copper coil (inductor), and then quenching by spraying of water or other fluids [16]. The essential issue is rapid heating, which shifts to higher values the start temperature for austenite formation (A_{c1}) and the temperature at which transformation of ferrite to austenite is completed (A_{c3}). More specifically, A_{c1} is a function of the heating rate, of the microstructure prior to induction hardening and of the chemical composition of steel [17]. For the outlet/inlet rocker arm and pushrods composed of hypoeutectoid carbon steels, the starting microstructures consisted of pearlite and proeutectoid ferrite. When A_{c1} is reached, these phases initiate the transformation into austenite, which occurs more rapidly in pearlite. The rates of austenitization depend on size and shape of the workpieces, so the final microstructure and grain size distribution will be non-uniform from the surface to the core of material [17]. Previous research showed that A_{c1} and A_{c3} temperatures were significantly higher for an initial microstructure of ferritic-pearlitic type than for a tempered martensitic one [18]. In the present study, for all pairs of rocker arms unsuitable austenitization temperatures and times left some of the proeutectoid ferrite untransformed, in the form of free ferrite. The presence of free ferrite was also probably favored by a design of the inductor shape unsuitable for the induction hardened regions, especially for those of the rocker arm pivot sockets. Improper austenitization parameters and/or unsuitable design of the inductor shape could therefore be responsible for the non-compliance with the required specifications for the induction hardening treatment.

For all components, the scanning electron microscope analyses revealed linear grooves and scratch marks which were mostly parallel and uniformly distributed over wide areas of the worn surfaces. These data suggest scuffing as the main failure mode. Scuffing is known to be promoted by the presence of free ferrite in the microstructure, while pearlite tends to retard it [19]. In boundary lubrication conditions, it is associated with the progressive desorption of the lubricant at the contact interface, depending on the interaction among polar constituents of lubricants and surfaces, and on the rate of destruction and reforming of protective oxides [19]. When scuffing occurs, a severe surface destruction process is established [20,21], as confirmed by the increase in Sa, Sq and Ssk parameters from fresh to worn surfaces in the present study. Concerning the worn surfaces of exhaust/intake valve stem tip, the material removal by scuffing at the rocker arm/valve interface could be accelerated by the large primary carbides surfacing at the contact interface, identified by optical microscope observations, and by the Sku values > 3.00, indicating a surface with sharp peaks and deep valleys [20].

The SEM/EDS analyses of the worn surfaces at the rocker arm/valve interface also revealed the presence of numerous pits with subsurface interconnected microcracks and fatigue striations. The pits contained wear particles in the form of spherical agglomerates identified as iron oxides by EDS analyses. Pitting is the consequence of fatigue affecting surfaces characterized by non-conformal contacts [22]. In these conditions, fatigue cracks may nucleate either at the surface or at stress concentration points at small depths below the surface, such as non-metallic inclusions, precipitates or pre-existing flaws, and/or soft spots in the microstructure, for example in regions where free ferrite is present. Cracks then propagate towards the interior of the material and eventually curve up, producing wear particles and pits [16,22]. Fatigue cracking has been identified by the presence of fatigue striations inside pits that indicate the periodic advance of the crack front during cyclic loading. In all surfaces, residues of lubricant additive containing sulfur, phosphorous, calcium and zinc were detected, attributable to Zinc Dialkyl Dithio Phosphate (ZDDP) anti-wear additives. Previous research showed that ZDDP additives may promote fatigue crack initiation by preventing surface roughness reduction during running-in, or by creating corrosion pits on the contact surfaces [23,24]. Due to the high pressure at these surfaces, the lubricant flows into cracks, exerting a pumping effect which increases the driving force for crack propagation [25].
Finally, in some narrow regions of the worn surfaces of pushrod ball ends and rocker arm pivot sockets, a series of ripples oriented along the direction of grooves were observed, generated by erosive cutting. For ductile materials, these ripples may be the product of free moving particles transported by the lubricant and wearing out the softer surface [19].

5. Conclusions

A failure analysis of rocker arms, pushrods and valves collected from a four-cylinder diesel engine for industrial cleaning machines was performed to investigate the causes of excessive wear occurring at the rocker arm/pushrod and rocker arm/valve interfaces, after only 1000 hours of engine operation. Based on the results, the following conclusions can be drawn:

- the non-uniform wear damage detected at the rocker arm/valve interface suggests a misalignment of the valves with respect to the valve seat inserts;
- improper austenitization parameters and/or unsuitable design of the inductor shape left some free ferrite at the induction hardened regions of the rocker arms and pushrods. This faulty procedure could be responsible for non-compliance with required specifications for the induction hardening treatment;
- the presence of free ferrite at the induction hardened regions of rocker arms favors the material removal by scuffing and the initiation of fatigue cracks at the rocker arm/valve interface. The propagation of cracks is promoted by the pumping effect exerted by the ZDDP anti-wear additives;
- at the rocker arm/pushrod interface the wear damage is caused by material removal by scuffing and probably also by erosive cutting caused by free moving particles transported by the lubricant.

Acknowledgements

The authors thank Dr Milvia Chicca for help in revising the manuscript. This work was supported by the Department of Engineering, University of Ferrara (Ferrara, Italy), grant n. 2238/2010.

References

[1] M. Priest, C.M. Taylor, Automotive engine tribology – approaching the surface, Wear 241 (2000) 53–65.

[2] M. Mackaldener, Simulations in engine design with focus on tribology, Proceedings of the 10th Nordic Symposium on Tribology, Nordtrib 2002, Stockholm, Sweden, (2002).

[3] R. Lewis, R.S. Dwyer-Joyce, G. Josey, Design and development of a bench test rig for investigating diesel engine inlet valve and seat insert wear, Proceedings of Austrib '98, Brisbane, Australia, (1998).

[4] S. George, S. Balla, M. Gautam, Effect of diesel soot contaminated oil on engine wear, Wear 262 (2007) 1113–1122.

[5] S. Antusch, M. Dienwiebel, E. Nold, P. Albers, U. Spicher, M. Scherge, On the tribochemical action of engine soot, Wear 269 (2010) 1–12.

[6] M. Gautam, K. Chitoor, M. Durbha, J.C. Summers, Effect of diesel soot contaminated oil on engine wear – investigation of novel oil formulations, Tribol. Int. 32 (1999) 687–699.

[7] P. Diatto, M. Anzani, L. Tinucci, G. Tripaldi, A. Vettor, Investigation on soot dispersant properties and wear effects in the boundary lubrication regime, Tribology Series 36 (1999) 809–819.

[8] E.A. Khorshid, A.M. Nawwar, A review of the effect of sand dust and filtration on automobile engine wear, Wear 141 (1991) 349–371.

[9] C. Spiegelberg, S. Andersson, Simulation of friction and wear in the contact between the valve bridge and rocker arm pad in a cam mechanism, Wear 261 (2005) 58–67.

[10] Z.W. Yu, X.L. Xu, Failure analysis of diesel engine rocker arms, Eng. Fail. Anal. 13 (2006) 598–605.

[11] M.M. Muhammad, M.C. Isa, M.S.D. Yati, S.R.S. Bakar, I.M. Noor, Failure analysis of a diesel engine rocker arm, Def. S&T Tech. Bull. 3 (2010) 78–84.

[12] K. Mollenhauer, H. Tschöke, Handbook of diesel engines, Springer–Verlag GmbH, Berlin, 2010.

[13] P. Forsberg, P. Hollman, S. Jacobson, Wear mechanism study of exhaust valve system in modern heavy duty combustion engines, Wear 271 (2011) 2477–2484.

[14] Y.S. Wang, S. Narasimhan, J.M. Larson, S.K. Schaefer, Wear and wear mechanism simulation of heavy-duty engine intake valve and seat inserts, J. Mater. Eng. Perform. 7 (1998) 53–65.

[15] L. Jelenschi, C. Cofaru, G. Sandu, M. Aleonte, State of the art of engine valve and tappet rotation, Bulletin of the Transilvania University of Braşov, Series I: Engineering Sciences 4 (2011) 19–24.

[16] G. Straffelini, Friction and wear. Methodologies for design and control, Springer International Publishing AG, Cham (ZG), Switzerland, 2015.

[17] B.J. Yang, A. Hattiangadi, W.Z. Li, G.F. Zhou, T.E. McGreevy, Simulation of steel microstructure evolution during induction heating, Mat. Sci. Eng. A 527 (2010) 2978–2984.

[18] K.D. Clarke, C.J. Van Tyne, C.J. Vigil, R.E. Hackenberg, Induction hardening 5150 steel: effects of initial microstructure and heating rate, J. Mater. Eng. Perform. 20 (2011) 161–168.

[19] R. Chattopadhyay, Surface wear. Analysis, treatment, and prevention, ASM International, Materials Park, Ohio, 2001.

[20] Y. Jeng, Impact of plateaued surfaces on tribological performance, Tribol. T. 39 (1996) 354–361.

[21] Y.S. Kang, C.H. Hager, R.D. Evans, Effects of skewed surface textures on lubricant film thickness and traction, Tribol. T. 58 397–406.
[22] A. Terrin, C. Dengo, G. Meneghetti, Experimental analysis of contact fatigue damage in case hardened gears for off-highway axles, Eng. Fail. Anal. 76 (2017) 10–26.
[23] A.A. Torrance, J.E. Morgan, G.T.Y. Wan, An additive's influence on the pitting and wear of ball bearing steel, Wear 192 (1996) 66–73.
[24] E. Lainé, A.V. Olver, M.F. Lekstrom, B.A. Shollock, T.A. Beveridge, D.Y. Hua, The effect of a friction modifier additive on micropitting, Tribol. T. 52 (2009) 526–533.
[25] B. L'Hostis, C. Minfray, M. Frégonèse, C. Verdu, B. Ter-Ovanessian, B. Vacher, T. Le Mogne, F. Jarnias, A. Da-Costa D'Ambros, Influence of lubricant formulation on rolling contact fatigue of gears – interaction of lubricant additives with fatigue cracks, Wear 382–383 (2017) 113–122.

FIGURE CAPTIONS

Fig. 1. Schematic representation of outlet/inlet rocker arm and parts of pushrod and exhaust/intake valve. The dashed lines enclose the regions with worn surfaces. A: outlet/inlet rocker arm pad. B: exhaust/intake valve stem tip. C: outlet/inlet rocker arm pivot socket. D: pushrod ball end.

Fig. 2. Stereomicroscopic images representing the excessive wear at the induction hardened regions: (a) outlet rocker arm pad; (b) inlet rocker arm pad; (c) exhaust valve stem tip; (d) intake valve stem tip; (e) outlet rocker arm pivot socket; (f) inlet rocker arm pivot socket. In (a) and (b) white arrows indicate the surface regions respectively located at the opposite directions of the intake and of the exhaust side, and in (a) the red and orange dashed lines enclose regions with different morphological features.

Fig. 3. Optical micrographs of the microstructure observed in cross-sections of the inlet rocker arm pivot socket. From the worn surface inwards: (a) induction hardened region with free ferrite (white areas); (b) transition region between the induction hardened layer and the unaffected core, with troostite (dark grey clusters) and free ferrite (white areas); (c) unaffected core.

Fig. 4. Optical micrographs of the microstructure observed in cross-sections of the intake valve stem tip. From the worn surface inwards: induction hardened region (a) and unaffected core (b) with primary and secondary carbides (white areas).

Fig. 5. Vickers hardness profiles of the cross-sections of inlet rocker arm pad (a), inlet rocker arm pivot socket (b), pushrod ball ends (c), exhaust valve stem tip (d) and intake valve stem tip (e), at a distance (mm) from the worn surfaces. Error bars represent standard deviation.

Fig. 6. The 3D isometric views of the worn surfaces of the outlet rocker arm pad (a), inlet rocker arm pad (b), exhaust valve stem tip (c) and intake valve stem tip (d).

Fig. 7. SEI-EM micrographs of the worn surface of pushrod ball ends: (a) overview of worn surface; (b) detail of the surface showing material removal by scuffing with parallel grooves and scratch marks; (c) detail of the surface showing erosive cutting with ripples oriented along the direction of grooves.

Fig. 8. SEI-SEM micrographs of the matted area with pits observed on the worn surface of outlet rocker arm pad: (a) overview of pits; (b) details of the subsurface of a pit showing interconnected microcracks and fatigue striations.

Fig. 9. SEI-SEM micrograph of a wear particle in form of a spherical agglomerate detected inside a pit of the matted area on the worn surface of outlet rocker arm pad (left) and semi-quantitative EDS analysis of the spherical agglomerate (right).

Fig. 10. SEI-SEM micrographs of the worn surface of an exhaust valve stem tip: (a) detail of grooves and scratch marks; (b) detail of pits.

Fig. 11. BSE-SEM micrograph of the worn surface of an intake valve stem tip (left) and semi-quantitative EDS analyses of dark (A) and light (B) contrast areas in the same surface (right).

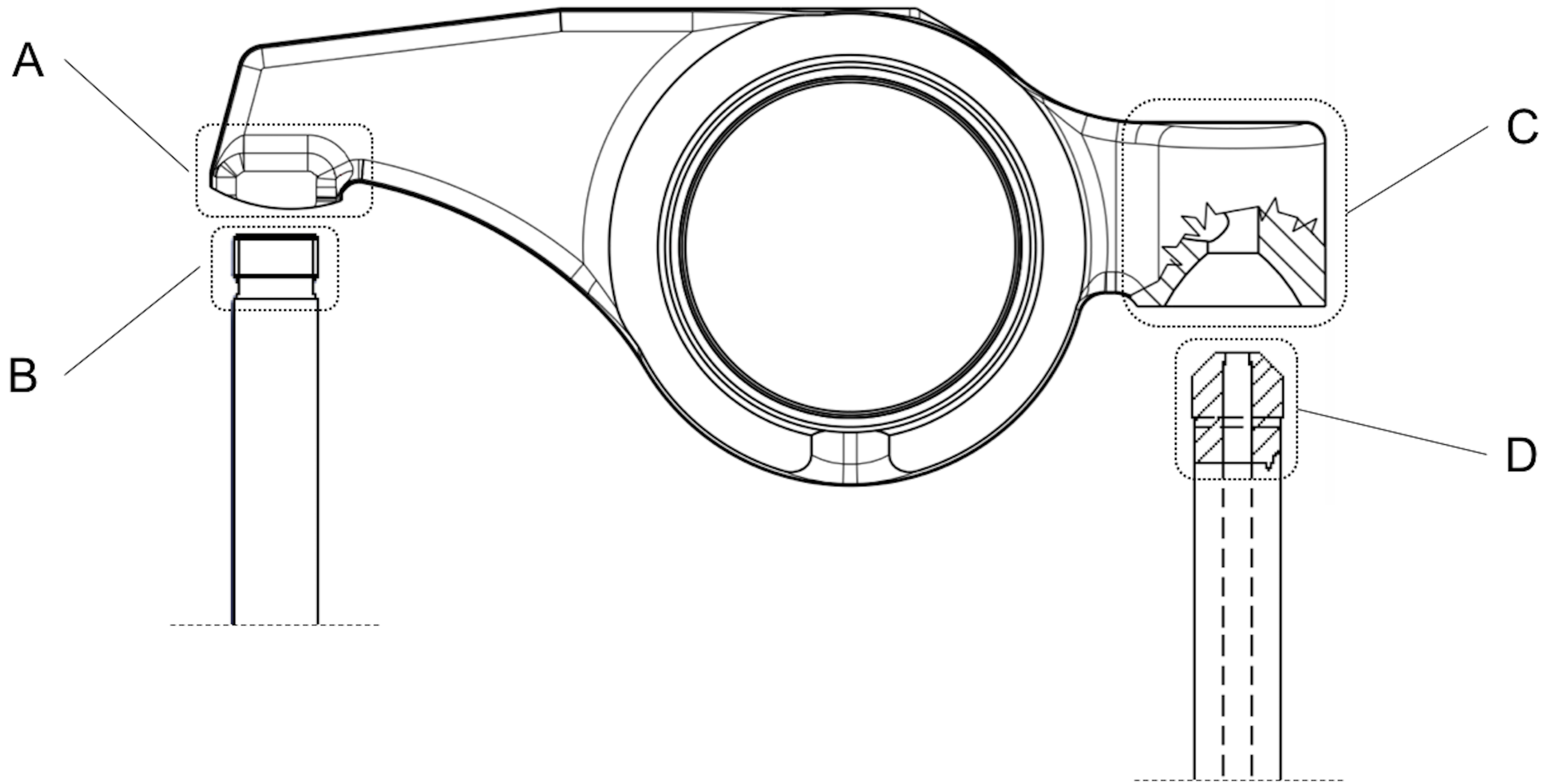
A
B
C
D

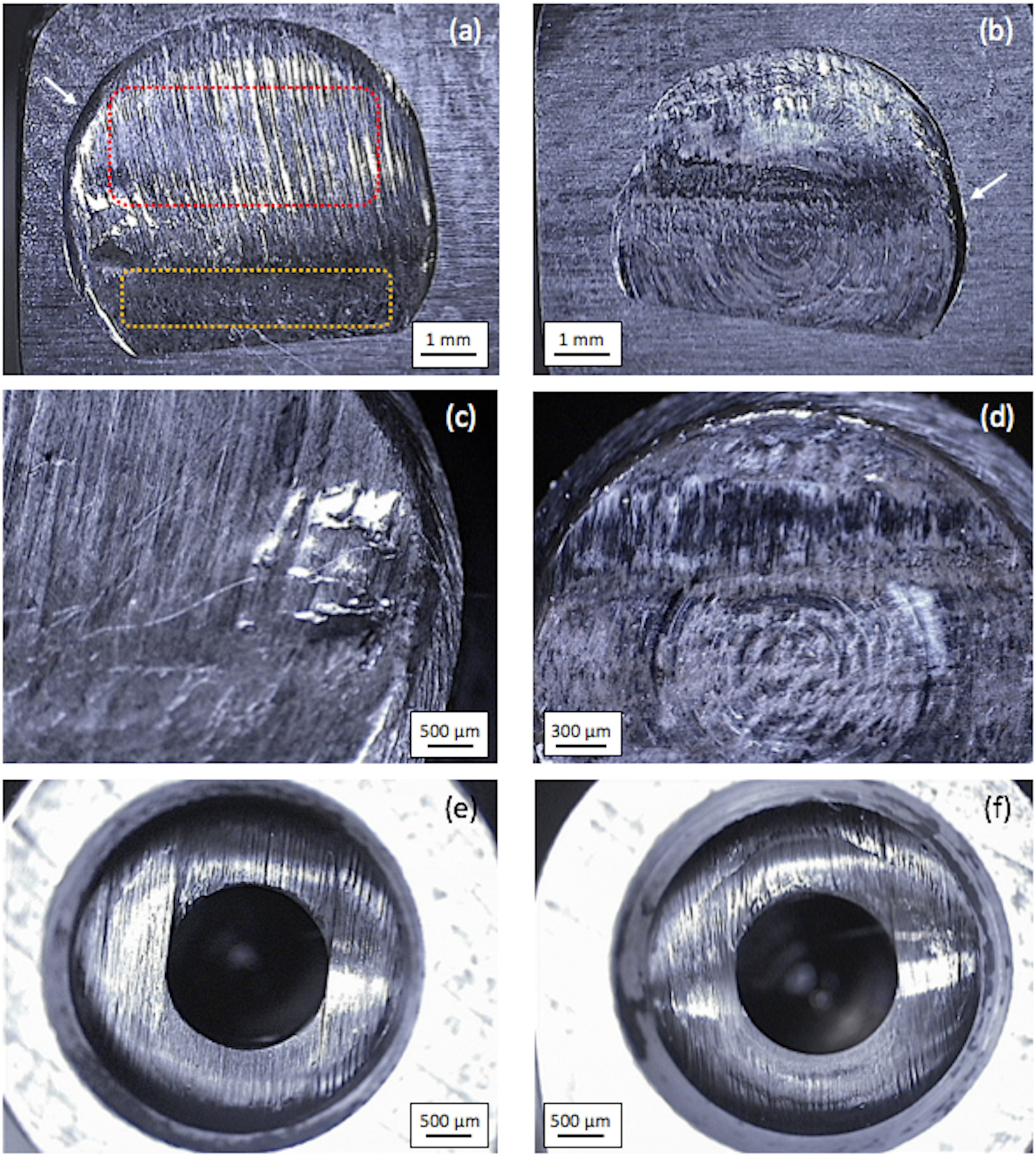
(a)
1 mm
(b)
1 mm
(c)
500 µm
(d)
300 µm
(e)
500 µm
(f)
500 µm

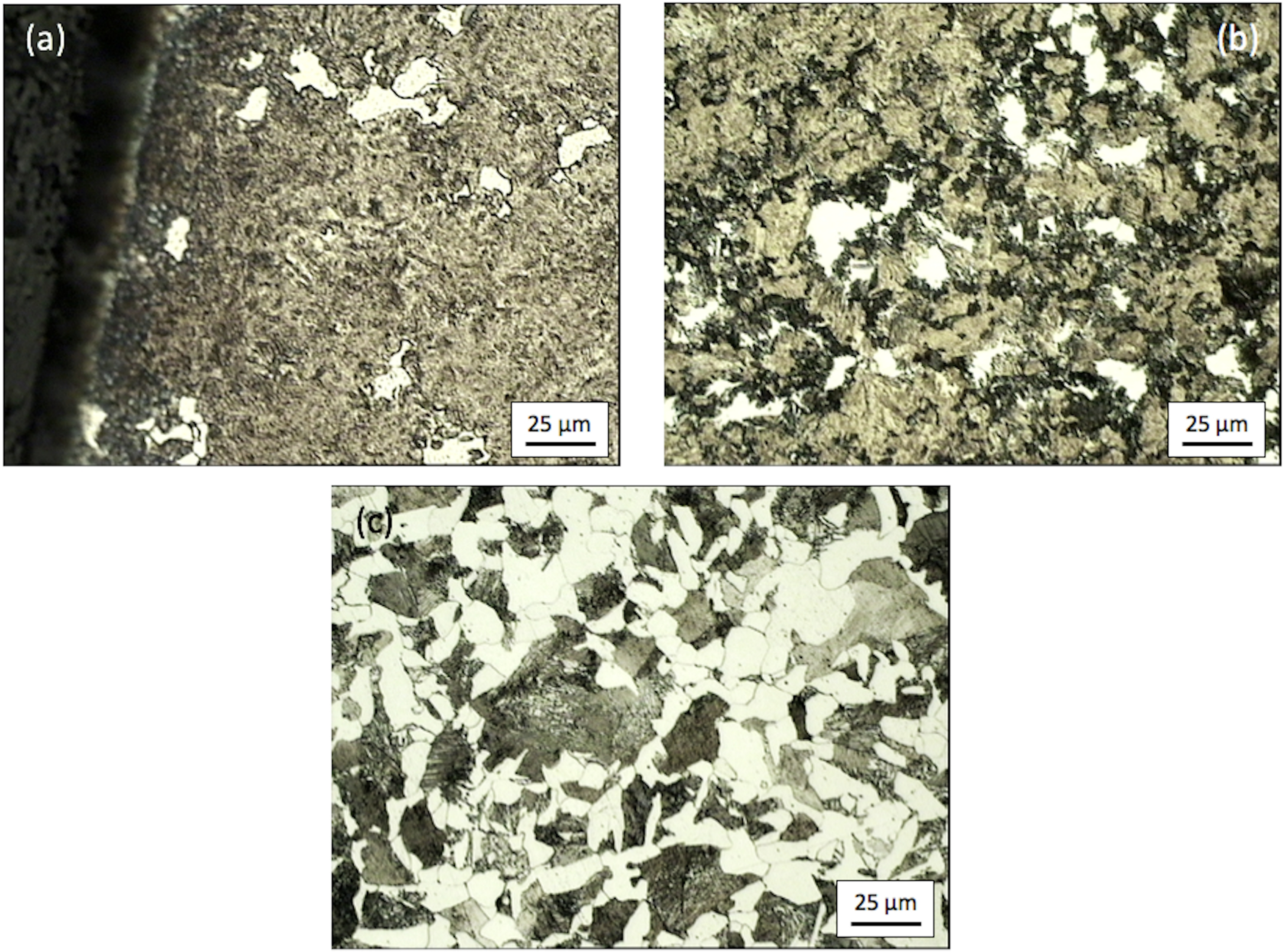
(a)
25 µm
(b)
25 µm
(c)
25 µm

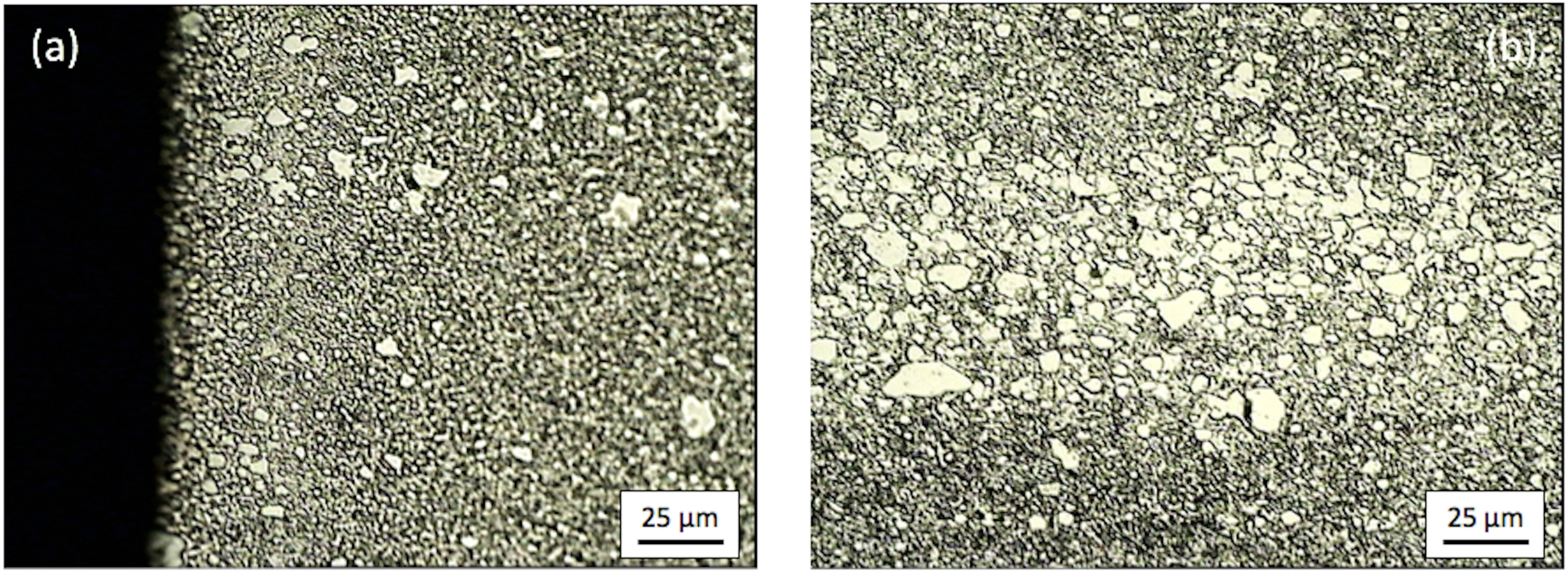
(a)
25 µm
(b)
25 µm

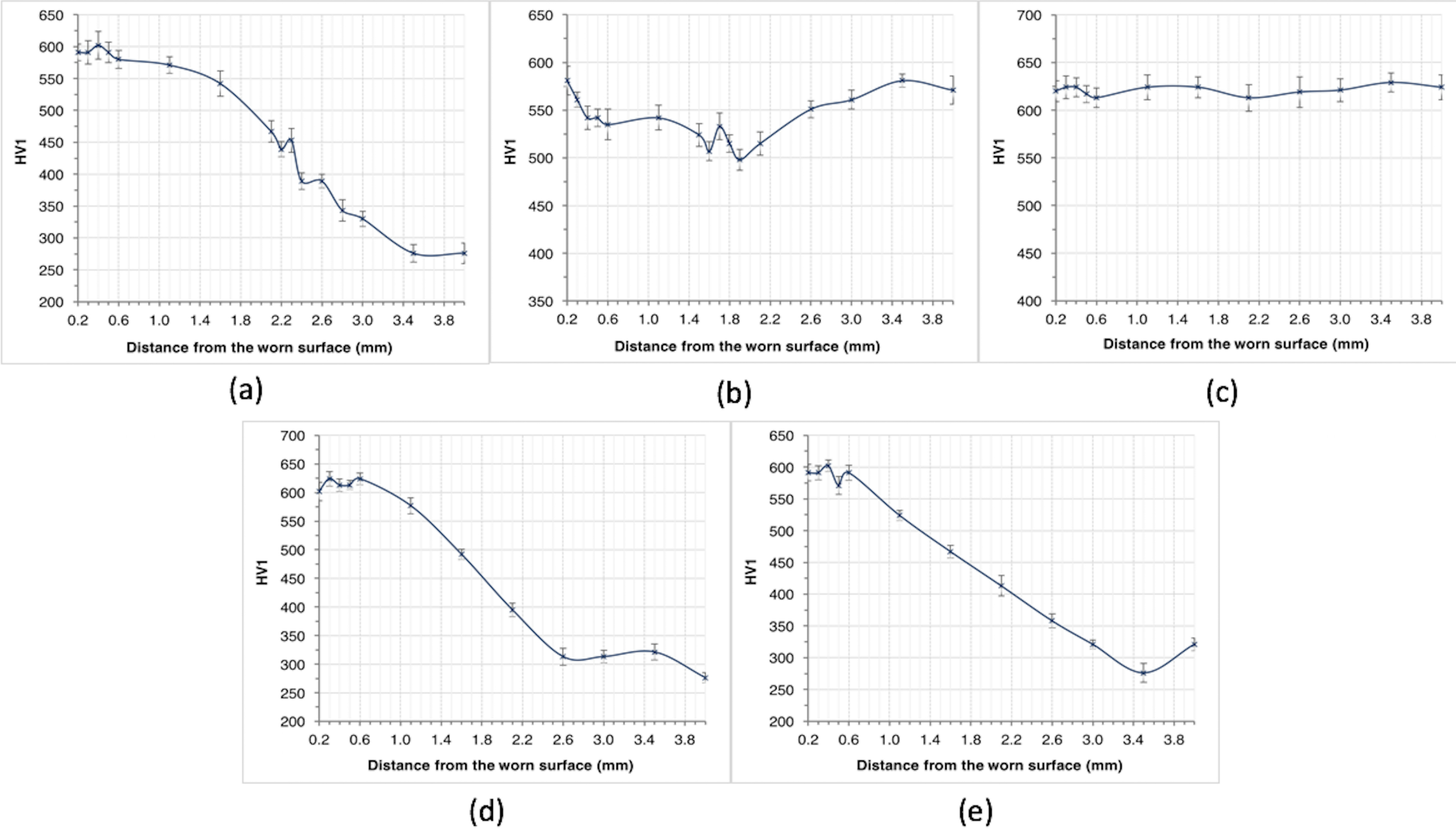
HV1
Distance from the worn surface (mm)
(a)
(b)
(c)
(d)
(e)

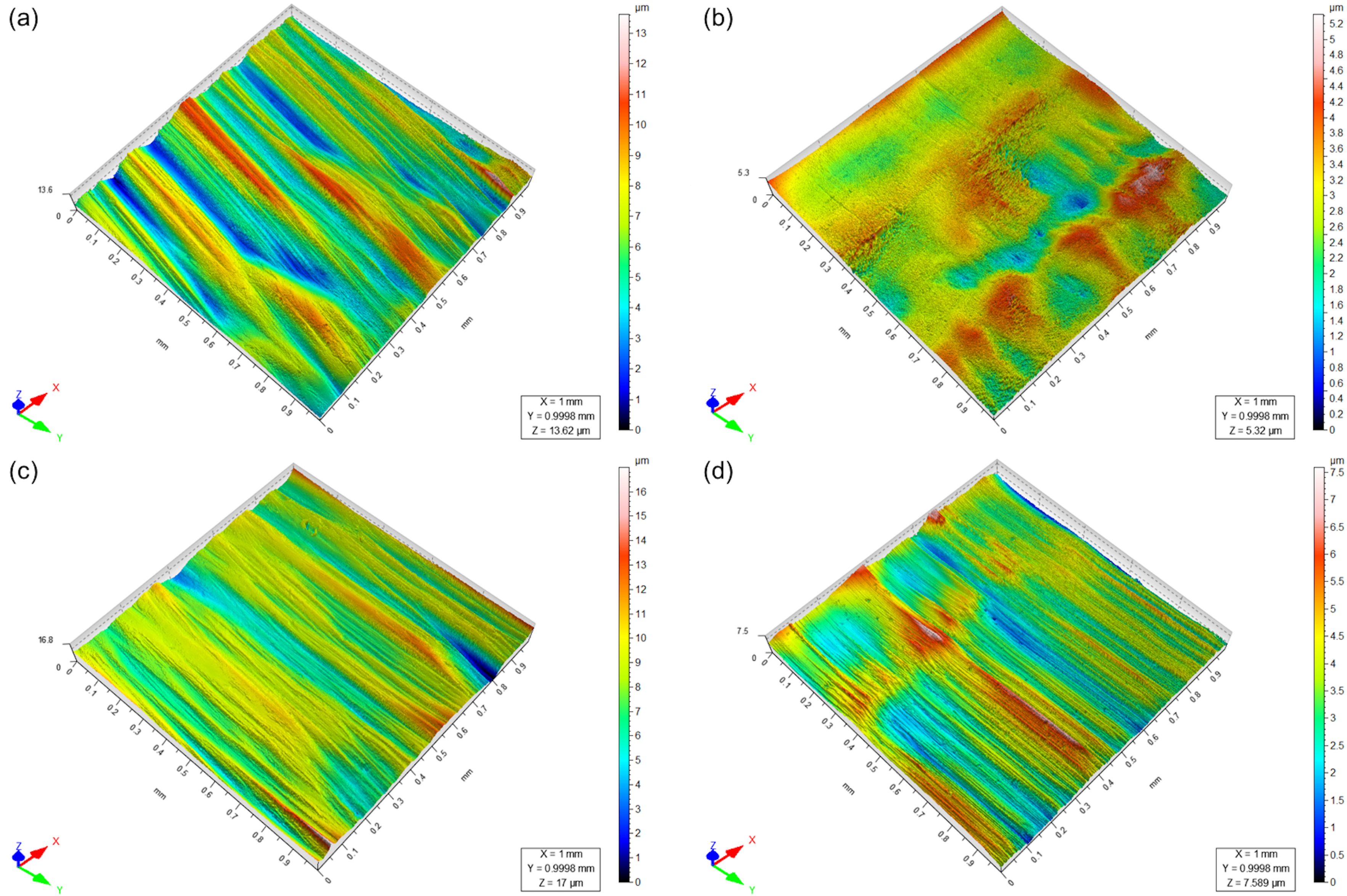

(a)
(b)
(c)
(d)
X = 1 mm
Y = 0.9998 mm
Z = 13.62 µm
X = 1 mm
Y = 0.9998 mm
Z = 5.32 µm
X = 1 mm
Y = 0.9998 mm
Z = 17 µm
X = 1 mm
Y = 0.9998 mm
Z = 7.589 µm
µm
mm

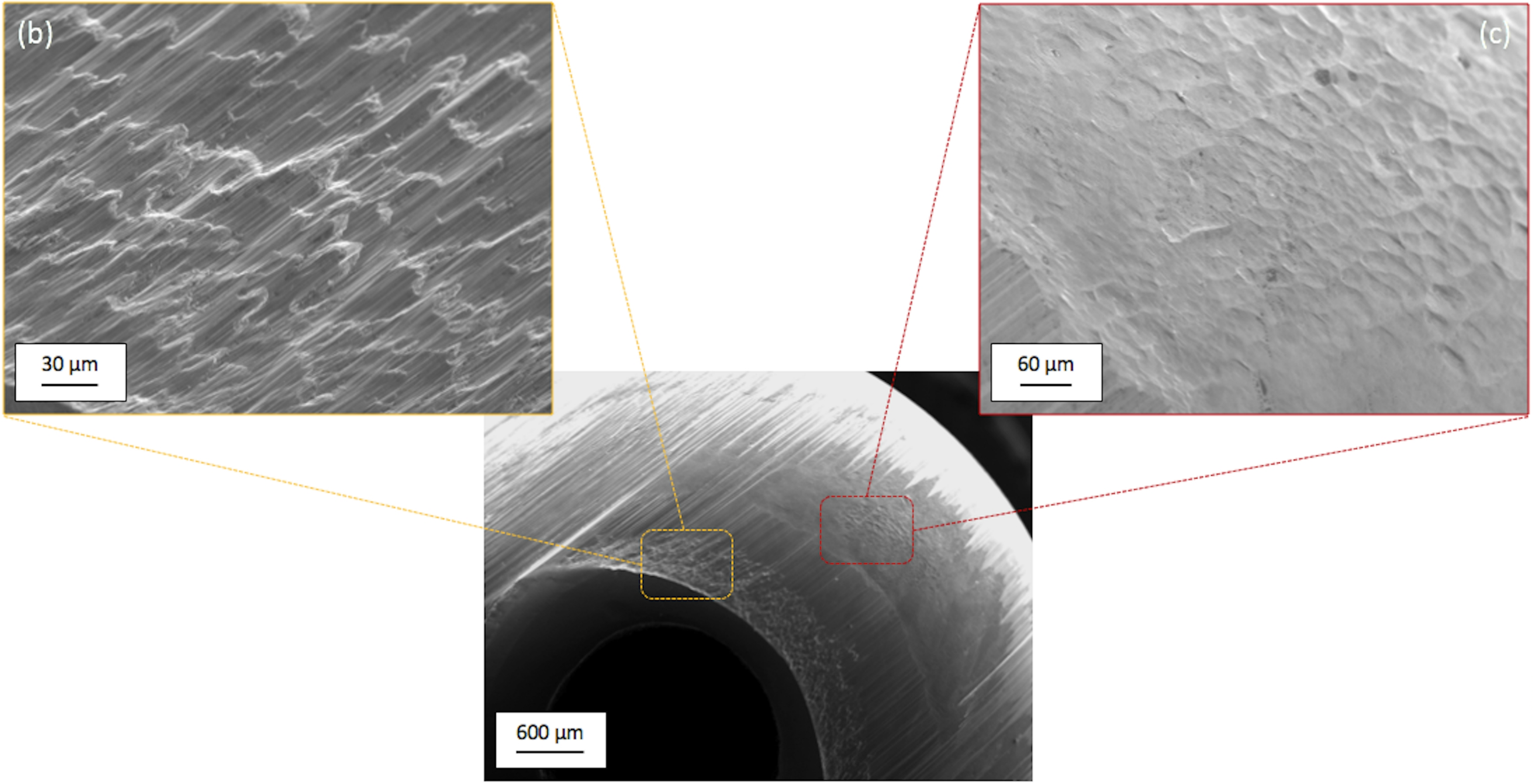

(a)

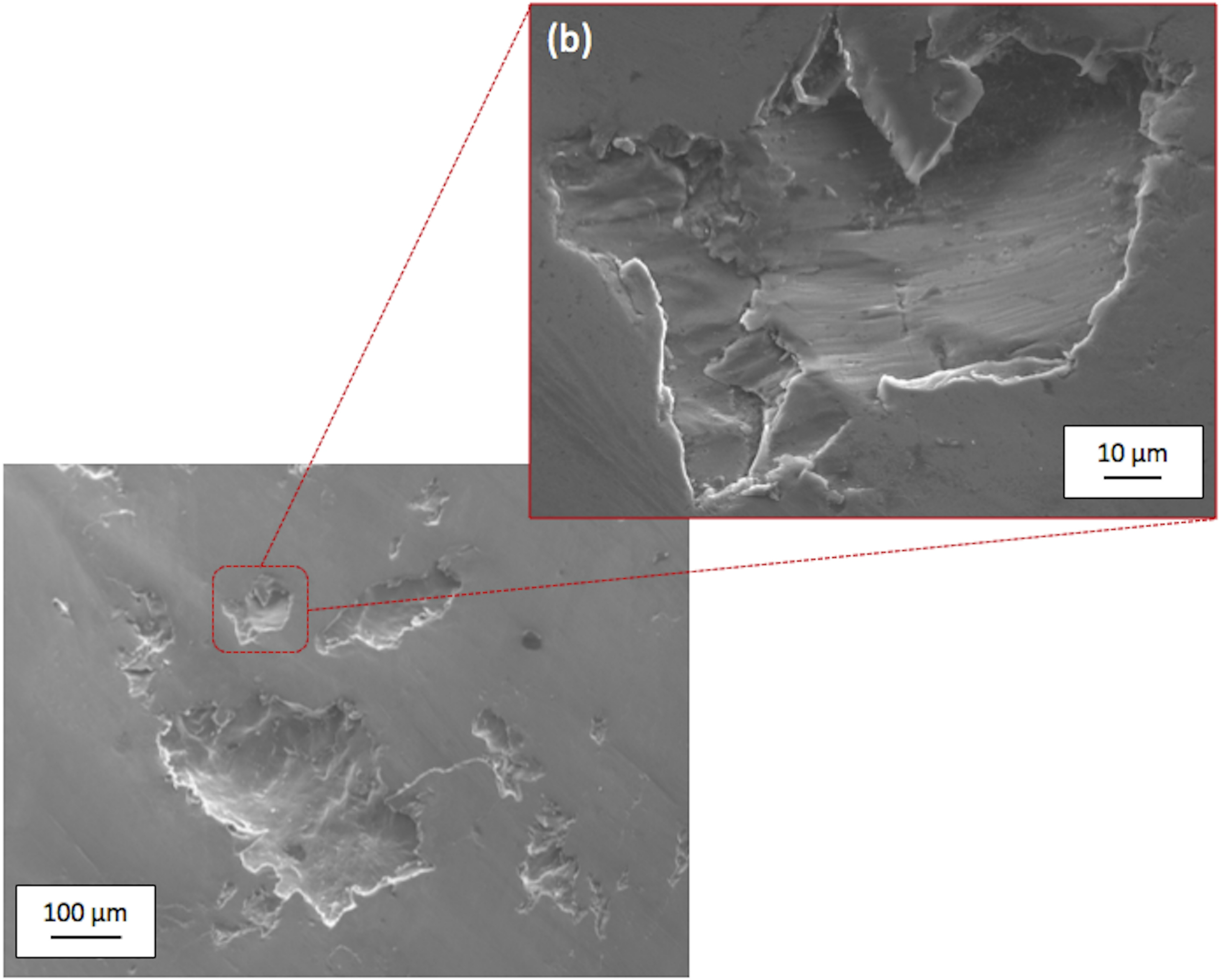

(a)

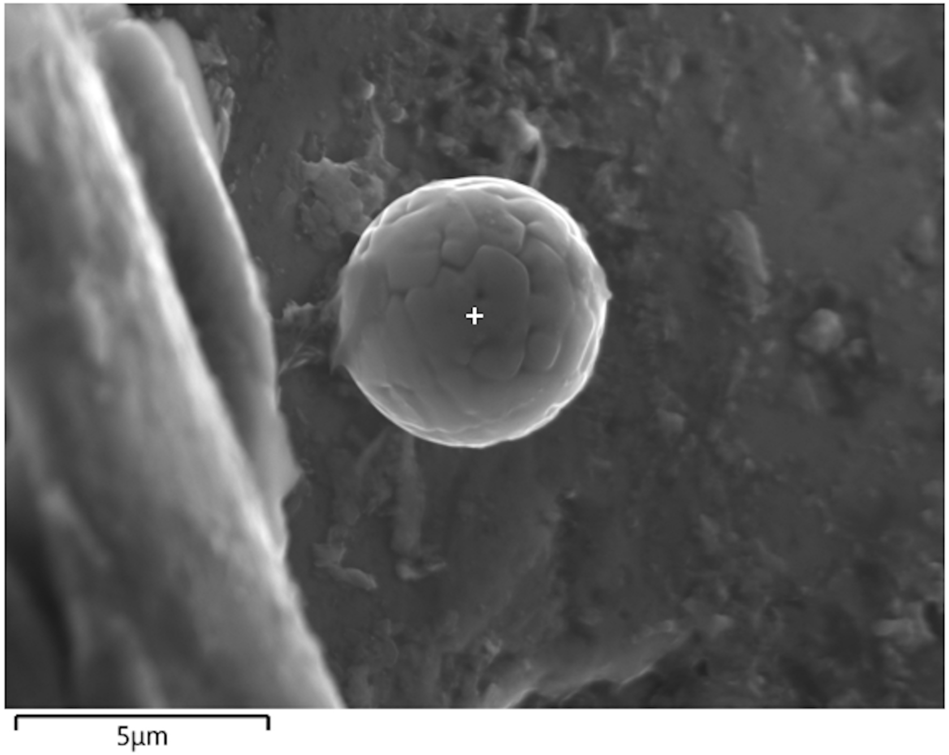
5µm

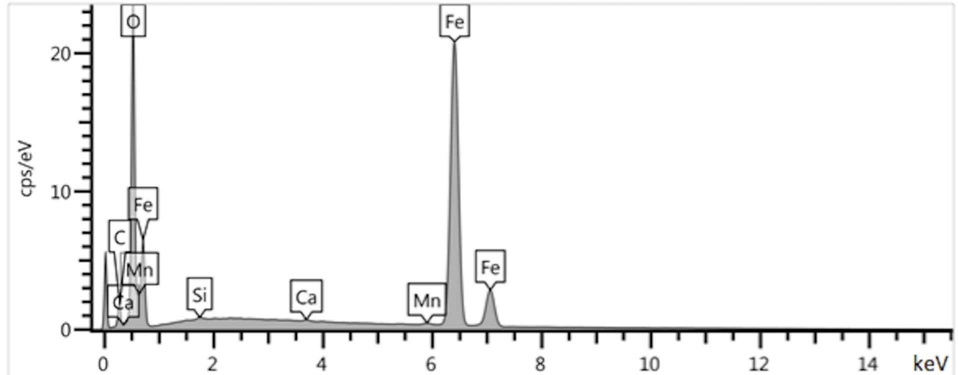
O
Fe
C
Fe
Mn
Ca
Si
Ca
Mn
Fe
cps/eV
20
10
0
0
2
4
6
8
10
12
14
keV

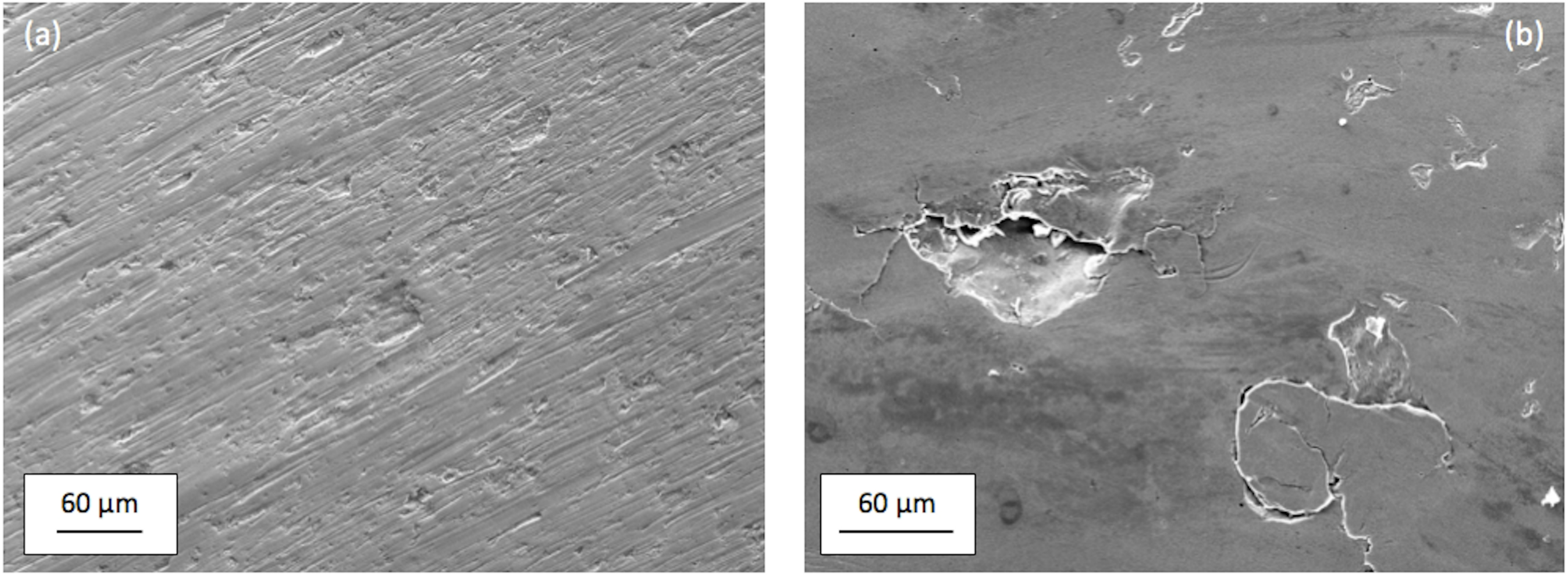
(a)
60 µm
(b)
60 µm

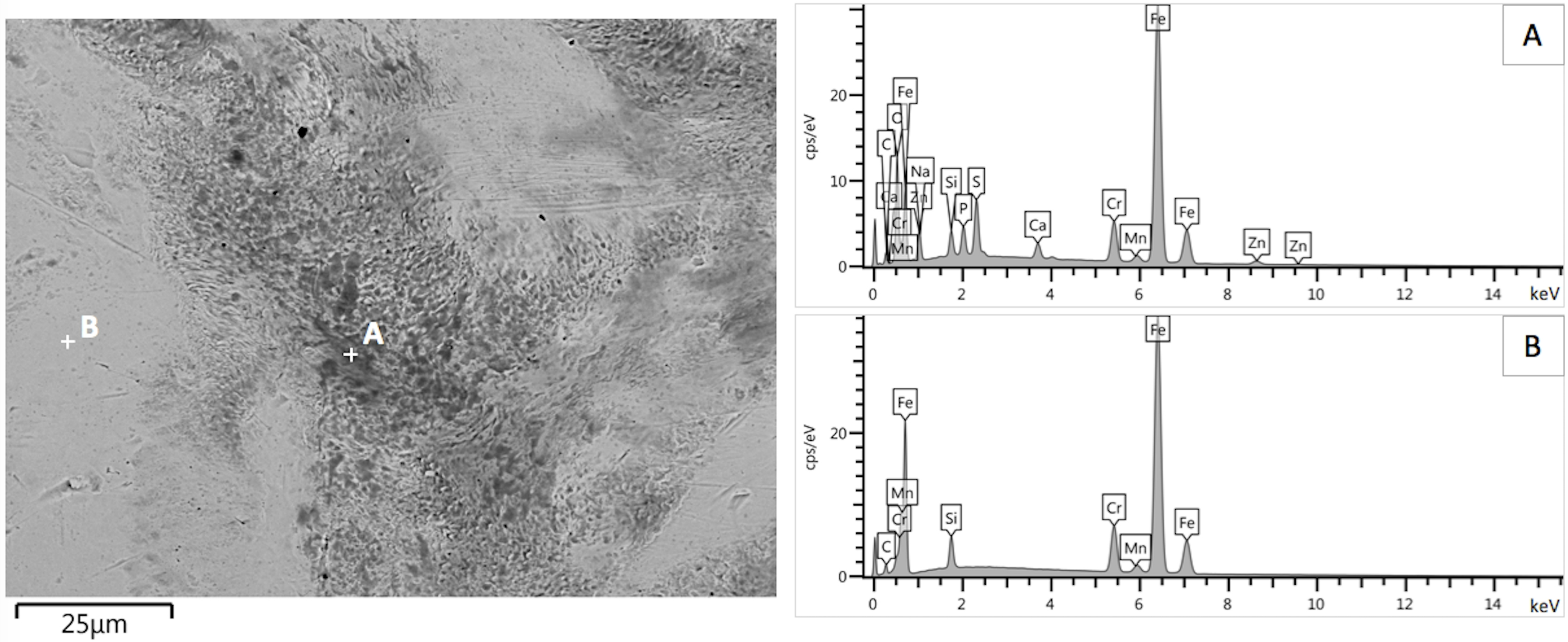

A
B
25µm
A
B
cps/eV
keV
Fe
C
Na
Si
S
P
Ca
Cr
Mn
Zn

Table 1 Chemical composition (wt%) of steel types of the worn components of a four-cylinder diesel engine for industrial cleaning machines.

Component	**C**	**S**	**Mn**	**Si**	**Cr**	**Ni**	**Mo**	**Cu**	**Fe**
Outlet/Inlet Rocker arm	0.42	0.020	0.71	0.16	0.13	0.08	< 0.03	0.17	balance
Pushrods	0.37	< 0.002	0.67	0.20	0.19	0.07	0.06	0.14	balance
Exhaust valve	0.50	0.006	0.47	3.34	7.68	0.13	0.03	0.03	balance
Intake valve	0.88	< 0.002	0.60	0.61	16.15	0.13	1.75	0.05	balance

Table 2 Required specifications concerning Rockwell hardness values (HRC) and effective depth (mm) of the regions undergoing induction hardening treatment.

Induction hardened region	**HRC**	**Effective depth (mm)**
Outlet/Inlet Rocker arm pad	55-59	2.0
Outlet/Inlet Rocker arm pivot socket	55-59	2.0
Pushrod ball ends	≥ 58	-*
Exhaust valve stem tip	≥ 54	0.8
Intake valve stem tip	≥ 48	0.8

* No effective depth could be established because the pushrod ball ends were totally induction hardened.

Table 3 Mean area fractions (%) ± standard deviation (SD) of bainite-martensite and free ferrite in the induction hardened regions of the outlet/inlet rocker arm pad, outlet/inlet rocker arm pivot socket and pushrod ball ends. Each area fraction was evaluated on wide areas (1.0x0.5 mm^2) of the cross-sections by image analysis software.

Induction hardened region	**Bainite-martensite**		**Free ferrite**	
	Mean	**SD**	**Mean**	**SD**
Outlet rocker arm pad	95.12	0.78	4.88	0.78
Inlet rocker arm pad	94.26	0.44	5.74	0.44
Outlet rocker arm pivot socket	90.10	0.97	9.90	0.97
Inlet rocker arm pivot socket	90.35	0.72	9.65	0.72
Pushrod ball ends	96.17	0.69	3.83	0.69

Table 4 Mean Sa (μm), Sq (μm), Ssk and Sku ± standard deviation (SD) of the fresh and worn surfaces of the outlet/inlet rocker arm pad and exhaust/intake valve stem tip.

Induction hardened region		Sa (μm)		Sq (μm)		Ssk		Sku	
		Mean	**SD**	**Mean**	**SD**	**Mean**	**SD**	**Mean**	**SD**
Outlet rocker arm pad	Fresh surface	0.78	0.07	1.00	0.09	-0.56	0.26	3.59	0.55
	Worn surface	1.49	0.26	1.81	0.30	0.14	0.21	2.57	0.21
Inlet rocker arm pad	Fresh surface	0.74	0.05	0.91	0.07	-0.42	0.14	2.87	0.42
	Worn surface	0.42	0.12	0.50	0.16	0.27	0.15	2.46	0.24
Exhaust valve stem tip	Fresh surface	0.63	0.05	0.81	0.08	-0.30	0.17	2.22	0.20
	Worn surface	1.16	0.21	1.47	0.30	-0.26	0.51	3.74	1.10
Intake valve stem tip	Fresh surface	0.65	0.04	0.86	0.05	-0.35	0.15	2.25	0.21
	Worn surface	0.72	0.13	0.90	0.14	0.18	0.40	3.10	0.45